New Mexico Geological Society

*Downloaded from:* https://nmgs.nmt.edu/publications/guidebooks/67




# *Fluvial terraces in the lower Rio Salado valley: correlations, estimated ages, and implications for Quaternary faulting and for surface uplift above the Socorro Magma Body*

Brad D. Sion, Gary J. Axen, Fred M. Phillips, and Bruce J. Harrison
2016, pp. 235-247. https://doi.org/10.56577/FFC-67.235

*in:*

*Guidebook 67 - Geology of the Belen Area*, Frey, Bonnie A.; Karlstrom, Karl E. ; Lucas, Spencer G.; Williams, Shannon; Zeigler, Kate; McLemore, Virginia; Ulmer-Scholle, Dana S., New Mexico Geological Society 67th Annual Fall Field Conference Guidebook, 512 p. https://doi.org/10.56577/FFC-67

*This is one of many related papers that were included in the 2016 NMGS Fall Field Conference Guidebook.*

## Annual NMGS Fall Field Conference Guidebooks

Every fall since 1950, the New Mexico Geological Society (NMGS) has held an annual Fall Field Conference that explores some region of New Mexico (or surrounding states). Always well attended, these conferences provide a guidebook to participants. Besides detailed road logs, the guidebooks contain many well written, edited, and peer-reviewed geoscience papers. These books have set the national standard for geologic guidebooks and are an essential geologic reference for anyone working in or around New Mexico.

### Free Downloads

NMGS has decided to make peer-reviewed papers from our Fall Field Conference guidebooks available for free download. This is in keeping with our mission of promoting interest, research, and cooperation regarding geology in New Mexico. However, guidebook sales represent a significant proportion of our operating budget. Therefore, only *research papers* are available for download. *Road logs*, *mini-papers*, and other selected content are available only in print for recent guidebooks.

### Copyright Information

Publications of the New Mexico Geological Society, printed and electronic, are protected by the copyright laws of the United States. No material from the NMGS website, or printed and electronic publications, may be reprinted or redistributed without NMGS permission. Contact us for permission to reprint portions of any of our publications.

One printed copy of any materials from the NMGS website or our print and electronic publications may be made for individual use without our permission. Teachers and students may make unlimited copies for educational use. Any other use of these materials requires explicit permission.

*This page is intentionally left blank to maintain order of facing pages.*

New Mexico Geological Society Guidebook, 67th Field Conference, Geology of the Belen Area, 2016, p. 235-247.



# FLUVIAL TERRACES IN THE LOWER RIO SALADO VALLEY: CORRELATIONS, ESTIMATED AGES, AND IMPLICATIONS FOR QUATERNARY FAULTING AND FOR SURFACE UPLIFT ABOVE THE SOCORRO MAGMA BODY

Brad D. Sion, Gary J. Axen, Fred M. Phillips, and Bruce J. Harrison

Depart of Earth and Environmental Sciences, New Mexico Tech, 801 Leroy Place, Socorro, NM 87801; bsion@nmt.edu

**Abstract**—The Rio Salado, southwest of Belen, is a large western tributary of the Rio Grande with a valley that is flanked by six major terrace levels. The presence of several Quaternary, rift-related normal faults and a mid-crustal magma layer beneath the Rio Salado valley provide an unusual opportunity to investigate the effects of various modes of tectonic deformation of the terraces. In this study, we mapped Rio Salado terraces using a commercial high-resolution DEM and digital color stereophotographs on a GIS workstation. The terraces were projected onto a vertical plane to construct longitudinal profiles. We employed the terrace nomenclature of existing 1:24,000-scale geologic maps, but divide Qte into two distinct terraces (Qte1 and Qte2). We estimated terrace ages of 346±123 ka (Qtg), 235±105 ka (Qtf), 160±86 ka (Qte1), 95±36 ka (Qtd), 52±39 ka (Qtc), and 7±5 ka (Qtb) using a net incision rate of 0.30±0.10 m/kyr, inferred from the correlation of Qte2 to the 122±18 ka Airport surface, ~25 km south of the Rio Salado valley. Terraces in the Loma Blanca fault (LBF) hanging wall are back-tilted relative to the footwall, suggesting a listric geometry for the LBF. Two exceptions are terrace levels Qtf and Qtc, which are east-tilted relative to their footwall counterparts. Both Qtf and Qtc merge eastward with the next youngest terrace in the flight. The Qtc terrace is arched, possibly reflecting surface uplift due to the Socorro magma body (SMB). Qtc is not offset by the LBF, suggesting that fault activity ceased in the valley prior to tread abandonment. This study is a preliminary report on the configuration and correlation of Rio Salado terraces. Future work will involve cosmogenic $^{36}$Cl surface exposure dating to obtain a quantitative chronology for the Rio Salado terraces and enable the determination of incision rates and improve correlation with terraces regionally. Surface exposure dates will also provide constraints on slip rates of Quaternary faults and the geologic history of the SMB.

## INTRODUCTION

The Rio Salado, southwest of Belen, is a large western tributary of the Rio Grande that originates in the Sawtooth Mountains and joins the Rio Grande ~140-km downstream at the southern edge of the Albuquerque basin near San Acacia, NM (Fig. 1). Much of the upper Rio Salado is carved in bedrock, but the lower 25 km occupy an alluvial channel incised into the Santa Fe Group. This reach of the Rio Salado is flanked by several terrace levels that were mapped and correlated by Machette (1978) and Majkowski (2009). We refine these earlier terrace correlations using new high-resolution longitudinal terrace-tread profile analyses. Additionally, we extend these correlations to well-documented terraces in the Rio Grande valley (Love et al., 2009) and major tributaries (Chamberlin, 1999; Goldstein, 2001). Correlation of a major Rio Salado terrace to an extensive fill terrace along the Rio Grande (the 30-m terrace of Love et al., 2009) provides fundamental age control for Rio Salado terraces. This correlation, together with integration of detailed terrace elevations, relative terrace positions in the flight and soil characteristics, permit preliminary age estimates for the terrace suite along the Rio Salado.

The term *terrace* requires a proper definition because of the complex processes involved in the formation and preservation of terraces and associated alluvial deposits. Terraces are geomorphic surfaces underlain by alluvial deposits and can be easily identified along river-valley margins by their diagnos-

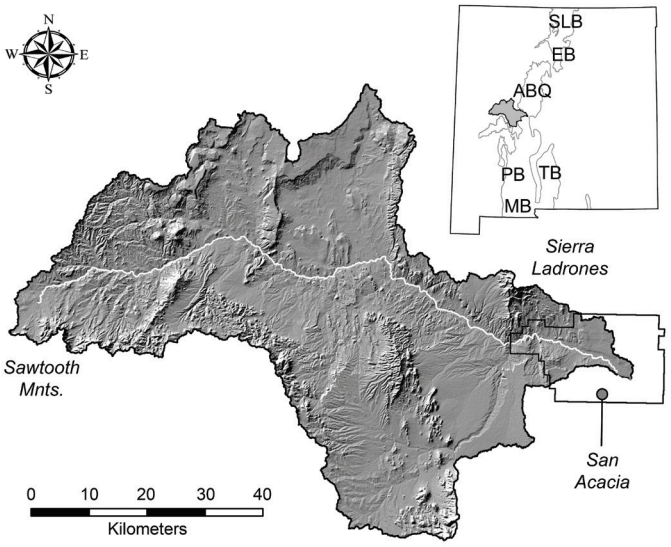



FIGURE 1. Location map of the Rio Salado watershed, central New Mexico. Shaded relief basemap derived from 30-m DEM. Rio Salado flows from west to east into the study area, outlined by the irregular black polygon. Abbreviations in the inset map of New Mexico indicate major rift basins. SLB = San Luis basin, EB = Española basin, ABQ = Albuquerque basin, PB = Palomas basin, TB = Tularosa basin, MB = Mesilla basin.

tic step-like appearance (e.g., Bull, 1990, 1991; Connell et al., 2007; Pazzaglia, 2013). Terraces are typically distinguished either as fill, fill-cut or strath terraces, depending on the thickness of the alluvial deposit beneath the low-relief upper surface (tread) and basal erosional surface (strath) (Bull, 1990, 1991; Connell et al., 2007; Pazzaglia, 2013). Fill terraces are characterized by thick alluvial deposits that bury the former valley floor, resulting from periods of aggradation followed by vertical incision into the stream alluvium. Fill-cut and strath terraces are both the result of lateral erosion and valley-floor widening followed by vertical incision, with the primary distinction that strath terraces are generally formed on bedrock and are commonly associated with tectonically active mountains (Bull, 1990, 1991; Pazzaglia, 2013).

Terrace chronology in New Mexico, and the Southwest in general, is typically presented in the context of a climate-response geomorphic model related to Quaternary glacial-interglacial cycles (Hawley, 1975; Hawley et al., 1976; Gile et al., 1981; Bull, 1990, 1991; Dethier and Reneau, 1995; Koning et al., 2011). This widely-accepted model suggests that the onset of glacial cycles correlates with increased river discharge accompanied by incision, that full-glacial conditions result in relative landscape stability primarily due to increased vegetative cover, and that increased aridity and decreased river discharge during the transition from glacial to inter-glacial periods promote erosion of highlands bordering the valley and aggradation of the valley floor (Hawley, 1975; Hawley et al., 1976; Gile et al., 1981; Love et al., 1987; Bull, 1990, 1991; Koning et al., 2011).

Although terraces are commonly used as indicators of Quaternary climate fluctuations, their utility as kinematic strain markers also allows workers to constrain rates and timing of tectonic activity. Tectonic uplift can have dramatic effects on terrace gradients and incision rates where uplift rates are rapid (Burbank and Anderson, 2011; Merritts et al., 1994; Wegmann and Pazzaglia, 2002; Riihimaki et al., 2007). For example, terrace studies in the Tien Shan in western China documented ~100 m of differential terrace uplift over the apex of actively-growing anticlines and established an age of ~25-35 ka for the onset of folding based on inferred surface uplift rates of ~1 mm/yr (Molnar et al., 1994). Rock uplift rates approaching 2 cm/yr were identified in central Nepal from fault-bend folding of fluvial terraces due to activity on the Main Frontal Thrust (Lavé and Avouac, 2000). Fault-slip rates were also identified from terrace ages and surface displacement on Ventura River terraces in California (Rockwell et al., 1984).

This paper utilizes Rio Salado terraces as tectonic strain markers to assess the magnitude and timing of vertical uplift above the Socorro magma body as well as the paleoseismicity of three normal faults within the Rio Grande rift. We primarily rely on terrace tread elevations, but strath elevations measured from exposures of one intermediate terrace level enhance the analysis. We recognize: (1) systematic changes in tread and strath heights of an intermediate terrace over the zone of maximum surface uplift above the Socorro magma body, and (2) the lack of apparent deformation of the tread of a lower inset terrace, indicative of a long history of magmatic activity. We also constrain the last slip event on the Loma Blanca fault and note changes in terrace tread gradients across the fault, suggestive of a listric geometry. We correlate Rio Salado terraces to a terrace suite along the Rio Grande (Connell, 2007; Love et al., 2009) in order to obtain age control for estimating stream incision rates and reconstructing the tectonic history. Of these Rio Grande terraces, the 30-m terrace of Love et al. (2009) is particularly important because it likely correlates to the Socorro Airport tributary terrace dated using the $^{36}$Cl depth-profile method (122±18 ka; Gosse and Phillips, 2001; Phillips et al., 2003).

## GEOLOGIC SETTING

The Rio Salado traverses a variety of bedrock lithologies before joining the Rio Grande. The upper and middle reaches of the Rio Salado valley are incised into Upper Triassic Chinle Group, Cretaceous marine and nonmarine rocks, Tertiary extrusive and intrusive rocks, and a variety of Paleogene sediments (Geologic Map of New Mexico, 2003). The lower ~30 km of the Rio Salado is incised primarily in Miocene Popotosa Formation and Plio-Pleistocene Sierra Ladrones Formation basin fill deposits of the Santa Fe Group (Machette, 1978).

A flight of six alluvial terrace deposits is inset into the maximum aggradational surface of the Santa Fe Group along the lower Rio Salado valley (Machette, 1978). Rio Salado terrace deposits consist of silty sand to sandy gravel that range in thickness from 3 to >22 m (Table 1; Machette, 1976). Gravel types are dominantly Pennsylvanian limestones and Tertiary volcanic rocks, but there is a small percentage of Proterozoic rocks (including granites) shed from the Sierra Ladrones to the north. The aggradational top of the Santa Fe Group is widely recognized throughout Rio Grande rift basins and is commonly used as a temporal datum because it marks the transition from regional aggradation to net incision of the Rio Grande and associated tributaries. The age of the aggradational top of basin fill deposits is constrained to ~800 ka in the Albuquerque Basin (Connell et al., 2013), which is consistent with the age of this surface in the Palomas Basin in southern New Mexico (Mack et al., 2006).

TABLE 1. Summary of terrace characteristics. Average linear terrace gradients are presented in both the footwall and hanging wall blocks of the Loma Blanca fault to illustrate changes across the fault.[1]From Machette (1978); [2]From Barns (2015).

| Terrace Level | Type | Thickness (m) | Average gradient (m/km) | |
|---|---|---|---|---|
| | | | Footwall LBF | Hanging wall LBF |
| Qtg | Fill | 6-15[1] | 5.4 | - |
| Qtf | Fill | 8-12 | 5.9 | 5.9 |
| $Qte_1$ | Fill | >22[1] | 5.6 | 4.2 |
| $Qte_2$ | Fill-cut? | >20.5[1] | 5.6 | 5.4 |
| Qtd | Fill-cut | 3-5[1] | - | 4.1 |
| Qtc | Strath | 3-6 | 6.0 | 7.8 |
| Qtb | Fill | <30[2] | 6.2 | 6.2 |
| Modern channel (alluvial reach) | - | - | 6.3 | |

We use longitudinal terrace-tread profiles in the lower Rio Salado valley to study the timing, rate and the style of Quaternary rift-flank faulting. The Loma Peleda, Loma Blanca and Cliff faults constitute the major Quaternary N-S rift-related normal faults in the lower valley (Machette, 1978; Figs. 2-3). The east-down Loma Peleda fault (LPF) extends for tens of km north and south of the valley. It offsets Holocene alluvium north of the valley but does not appear to offset post-Sierra Ladrones terraces in the lower Salado valley. It exhibits relatively steep (60-70°) dips north of the valley, but dips 28° south of the valley near Loma Blanca (Machette, 1978). The east-down Loma Blanca fault (LBF) can be traced for tens of km to the north and south, produces large scarps on several Quaternary alluvial units within the valley, and exhibits moderate (~45°) dips where the cemented fault plane is exposed. The west-down Cliff fault (CF) can be traced for ~7.5-km south of the valley and ~14-km north of the valley. It is well-expressed south of the valley near the San Acacia dam, where Neogene basalts (4.87±0.04 Ma; Chamberlin, 2001) in the footwall are juxtaposed against Quaternary alluvial deposits in the hanging wall. One dip measurement (60°) was reported by Machette (1978).

The Socorro magma body (SMB; Fig. 2), a thin (~100 m) tabular sill located at 19-km depth ~45 km southwest of Belen beneath Socorro County, is the world's second-largest (~340 km$^3$) known active magma body. Railroad leveling, satellite interferometry and GPS surveys show vertical and horizontal land surface motions with maximum vertical rates up to 2.5 mm/yr in a dome-like fashion above the SMB in the vicinity of the lower Rio Salado valley (Reilinger et al., 1980; Larsen et al., 1986; Ake and Sanford, 1988; Fialko and Simons, 2001; Finnegan and Pritchard, 2009; Pearse and Fialko, 2010; George et al., 2012). Maximum vertical surface velocities are located at Cerritos de las Minas, a few kilometers south of the Rio Salado valley (Fig. 2). Railroad leveling surveys dating back to the early 1900s indicate that the SMB has been active for at least 100 years (Reilinger and Oliver, 1976; Reilinger et al., 1980). Details regarding the emplacement and evolution of the SMB are lacking, but 1-D thermal modeling suggests that a magma body of this thickness and depth should completely crystallize on a 1-kyr timescale if instantaneously emplaced (Finnegan and Pritchard, 2009). The presence of the SMB provides us with an unusual opportunity to investigate terrace response to long-wavelength, relatively low-amplitude uplift signals, constrain the age of SMB emplacement and interrogate deep magmatic processes.

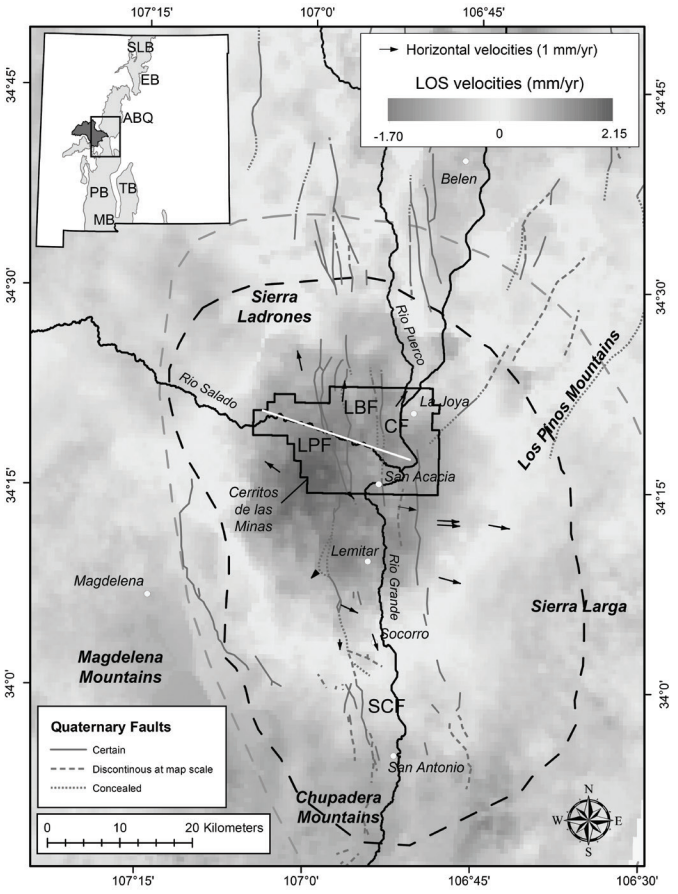



FIGURE 2. Location map of major Quaternary normal faults, outline of the Socorro magma body (SMB), and outline of the Socorro seismic anomaly (SSA). Basemap indicates Line of Sight (LOS) surface velocities from InSAR satellite data (from Pearse and Fialko, 2009). Arrows indicate horizontal ground velocities from GPS measurements (George et al., 2012). The zone of maximum surface uplift is located a few kms south of the study area (black polygon), in the northern two-thirds of the SMB. The average trend of the Rio Salado valley used for projecting the terrace data is shown for reference.

## PREVIOUS WORK

The Quaternary geology of the lower Rio Salado has been improved by several workers since Denny (1941) produced the first Quaternary geologic map of the area. Denny (1941) initially identified pediments of Tio Bartolo (75-m surface) and Valle de Parida (45-m surface) age in the lower Rio Salado valley, but lumped the majority of Quaternary deposits into a single, undifferentiated unit. Machette (1978) mapped subunits of piedmont and alluvial deposits and identified eight allostratigraphic units. These consist of alluvial fan, alluvial flat, pediment and terrace deposits (Machette, 1978). Majkowski (2008) mapped terrace-tread remnants on the south flank of the Rio Salado valley west of the interstate, measured their relative heights from the streambed using a Jacob staff, and studied their soil development to improve the terrace correlations of Machette (1978).

Several studies have attempted to assess the magnitude of SMB-related surface uplift using river terraces and longitudinal river profiles. Ouchi (1985) examined six longitudinal profiles of the Rio Grande and identified a convexity located in the zone of maximum surface uplift that he attributed to magma-body inflation. Finnegan and Pritchard (2009) examined longitudinal river profiles of the Rio Puerco and Rio Salado, two large tributaries that contribute a majority of Rio Grande sediment (Gellis et al., 2004), and concluded that the lack of a similar bulge in the profiles of these tributaries suggests that sedimentary processes were responsible for the Rio Grande bulge. Love et al. (2009) examined terrace tread elevations of a prominent "30-m terrace" along the Rio Grande from Veguita, NM to Socorro, NM and did not identify SMB-related deformation, concluding that either the SMB arrived recently

(< 1 kyr), magma injection has recently accelerated, doming is due to a shallower and smaller magma body, or episodic doming and relaxation has resulted in little net uplift. Majkowski (2008) constructed a longitudinal profile of Rio Salado terrace remnants and concluded that the terrace-tread heights increase over the zone of maximum SMB-related uplift. She overlooked prominent terrace surfaces on the northern flank of the valley and those east of I-25 on the southern flank, however, and her correlations were based on a limited number of terrace-height measurements, prompting additional investigation.

## TERRACE MAPPING AND CORRELATION

### Procedures/Methods

Treads of terrace remnants were mapped on high-resolution, digital, color stereophotographs obtained from the New Mexico Bureau of Geology and Mineral Resources using 3D visualization software (Figs. 3-4). A high resolution DEM derived from airborne radar topographic mapping with 5-m point spacing and ≤1-m vertical accuracy (acquired from NEXTMap®) was used to construct longitudinal terrace profiles from the terrace tread maps (Fig. 5). Profiles were constructed by orthogonally projecting terrace-point elevations to the trend of the Rio Salado valley (Fig. 2), which were smoothed using an overlapping boxcar averaging technique and normalized using the modern streambed as a datum. Strath heights above the modern riverbed were measured in the field, where exposed beneath remnants of one intermediate terrace level (Qtc), using a handheld laser rangefinder. Terrace-tread remnants were correlated to previously identified terrace levels within the Rio Salado valley on the basis of existing geologic maps (Table 2; Machette, 1978; Majkowski, 2008), soil properties (e.g., pedogenic carbonate content), height above the modern channel and relative positions in terrace flights.

### Potential Correlation Problems

It is important to recognize that terrace correlations made on the basis of any of the properties mentioned above can be problematic for a variety of reasons, but integration of these and other properties serve to strengthen the terrace correlations. Pedogenic carbonate content, and quantification of soil properties in general, greatly depends on the accurate identification of the soil "parent material." In the arid Southwest, $CaCO_3$ fluxes into the soil profile primarily originate from eolian dust that is deposited on the terrace surfaces. In this case, the soil profile may contain multiple parent materials and calcic horizons (e.g., alluvial and eolian deposits) that may record different depositional histories. The use of terrace-tread elevations may also be problematic, especially when one is attempting to correlate terrace remnants that are widely spaced or affected by post-depositional deformation.

For example, a terrace tread may be buried by sheetwash, eolian material or alluvial fans exiting tributary drainages, and may also be eroded or dissected by gullying. These problems can be overcome by augmenting terrace-strath data, however, strath exposures may not be present and may themselves exhibit varying amounts of relief (Love et al., 2009). The position of a particular terrace level in a flight can be useful for correlation within a given tributary valley, but potential for asynchronous terrace development in different river valleys (Pazzaglia and Wells, 1990) complicates this correlation method, especially when comparing river valley systems with different tectonic histories. Autogenic complex-response terraces do not require external forcing and may further complicate correlations (Schumm and Parker, 1973; Bull, 1990; Pazzaglia, 2013).

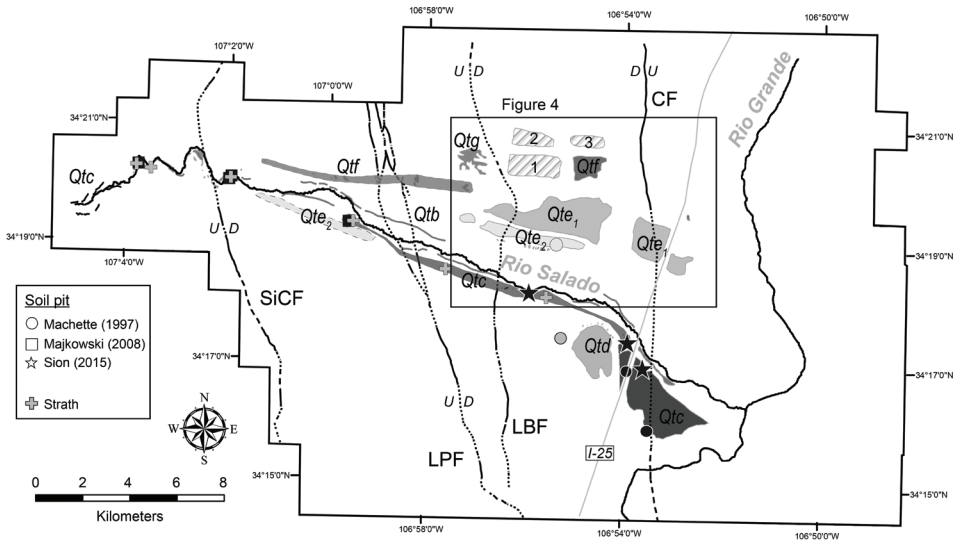



FIGURE 3. Terrace-tread map of the lower Rio Salado valley. Terrace Qtb is youngest and Qtg is oldest. Translucent shaded polygons connect small terrace-tread remnants that may not be visible at current map scale. Detailed location and elevation data (derived from dataset shown in Figure 4) were extracted within the individual terrace-tread polygons and projected to the trend of the valley (white line in Figure 2). Soil pit locations are given by circles, squares and stars, indicating the source where they were originally described. Soil pits are colored based on the surface on which they are dug. Crosses indicate locations where strath measurements were made on terrace Qtc. Inset box indicates the location of Figure 4.

## TERRACE STRATIGRAPHY AND FAULT RELATIONS

Six major terrace levels were differentiated in the lower Rio Salado valley (Qtb-Qtg) and consist of both fill and fill-cut terraces. Our nomenclature follows that of Machette (1978), where Qtb is the youngest/lowest terrace, and Qtg is the oldest/highest terrace (Table 2), but we lump his alluvial (Qa-) and piedmont (Qp-) deposits into our terrace nomenclature. In general, the terraces in the valley are preserved in longitudinally discontinuous erosional remnants. Terrace preservation is better within 10 km of the Rio Grande junction than

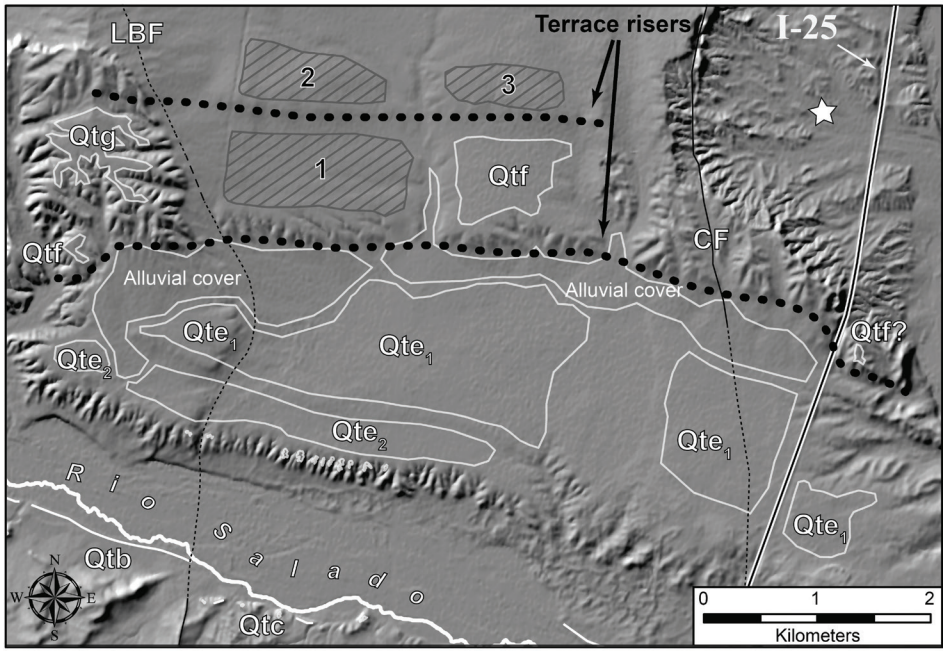



FIGURE 4. Large-scale map of terraces on the northern flank of the Rio Salado valley from inset box in Figure 3. Hillshade derived from a high-resolution (5-m pixels, 1-m vertical accuracy) DEM from NEXTMap® is shown as the basemap. Thin white lines and unfilled polygons represent terrace tread boundaries. Geomorphic surfaces labeled 1-3 are discussed in Sion (2015). Faults are indicated by thin dotted, dashed, and solid lines where the fault contact is respectively buried, inferred, or certain. Colluvial and eolian material generally cover the LBF fault contact and the fault is delineated with a dotted line even though prominent scarps are apparent. Black thick dotted lines indicate locations of terrace risers. White star indicates location of the Sevilleta National Wildlife Refuge headquarters.

farther upstream where the valley is narrower: only small discontinuous terrace treads are preserved upstream. A summary of the various terrace levels and associated thicknesses are presented in Table 1.

Qtb is the lowest and youngest Rio Salado terrace in the valley. It is a fill terrace parallel to and approximately 1 to 6 m above the modern channel within the study area. The thickness of Qtb fill is unknown, but results from a resistivity survey in the valley indicate that the fill may be up to 30 m thick (Barnes et al., 2015). Qtb deposits exposed along the valley flanks consist primarily of silt but coarsen to pebbly sand near the base at the elevation of the modern channel. Coarser deposits are exposed near the junctions of Cañada Popotosa and Arroyo Tio Lino (Fig. 5), two relatively large tributaries of the Rio Salado. Qtb deposits bury the LPF, LBF and CF (Machette, 1978). Cut-bank soil exposures indicate little pedogenic carbonate accumulation (Stage I; Table 2) and early stages of oxidation, suggestive of a Holocene age. A similar terrace level (T4; ~4 m above the channel) in Socorro Canyon to the south also has little pedogenic carbonate accumulation and thus is interpreted is a late Holocene terrace (Goldstein, 2001; Phillips et al., 2003).

Qtc forms a minor strath terrace with a tread height that ranges from 4-18 m above the modern channel. It is preserved as small, discontinuous remnants located on the southern valley flank. The terrace alluvium is generally 3-6 m thick and consists of sub-angular to sub-rounded pebbly sand to sandy gravel. The basal strath was identified in six localities (Figs. 3 and 5), overlying Popotosa Formation in the upper 5 km, Sierra Ladrones Formation around 14 km,

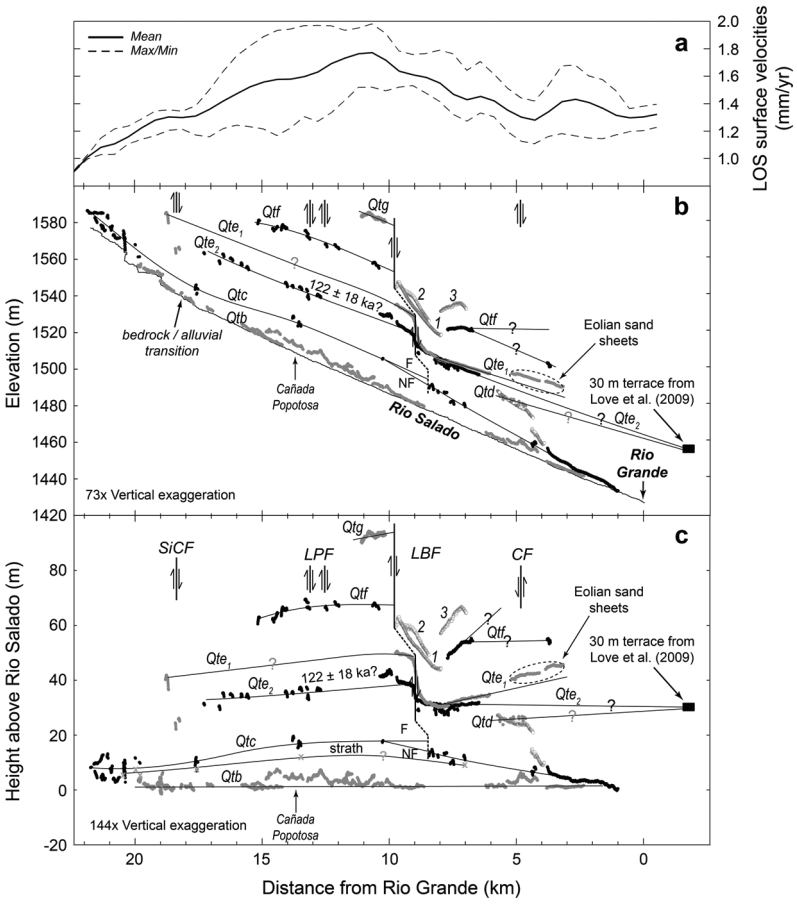



FIGURE 5. Plots of average surface velocities above the Socorro magma body (panel **a**) and longitudinal terrace-tread profiles (panels **b** and **c**). Terrace-tread profiles were created by projecting terrace-point elevations to a 2-D plane parallel to the average valley trend (Fig. 2) and smoothing the resulting point clouds with a moving boxcar averaging technique. The longitudinal terrace-tread profile was normalized (panel **c**) to modern channel gradient to emphasize tectonic deformation of terrace treads. Strath elevations measured from exposures beneath Qtc are indicated with gray x's. The strath surface is visually interpolated between each measurement. Faulted (F) and non-faulted (NF) reconstructions of the Qtc tread are presented, but we prefer a non-faulted reconstruction (see text).

TABLE 2. Comparison of terrace nomenclature used in this paper with that of previous workers. Majkowski (2008) used numbers to indicate relative terrace age. Her oldest terrace is indicated by a 1 and she uses increasing numbers with decreasing terrace age. This paper uses the lettering nomenclature employed by Machette (1978). In this system, the letter "a" refers to the modern stream alluvium and lettering progresses with increasing terrace age. Our nomenclature includes both alluvial "Qa-" and piedmont "Qp-" deposits mapped by Machette (1978).

| This paper | Majkowski (2008) | Machette (1978) |
|---|---|---|
| Qtg | - | Qpg |
| Qtf | - | Qaf/Qpf |
| $Qte_1$ | - | Qae/Qpe |
| $Qte_2$ | Qt1 | Qae/Qpe |
| Qtd | Qt1 | Qpd |
| Qtc | Qt5, Qt6, Qt7 | Qac |
| Qtb | Qt8 | Qab |

and piedmont slope deposits (Tsp of Machette, 1978) in the lower 9 km. Both the strath and the tread appear arched relative to the modern channel and the terrace merges downstream with terrace Qtb near the confluence with the Rio Grande. A small-displacement, east-down normal fault is present in a cut-bank exposure of Qtc deposits ~1-km east of the LBF; however, this small-displacement fault cannot be proven to cut the tread of Qtc. It is possible that the LBF offsets the Qtc tread, therefore both faulted (F) and non-faulted (NF) reconstructions of Qtc are presented in Figure 5 for comparison. The age of Qtc is unknown, but Machette (1978) inferred a late Pleistocene age. Soils on remnants of Qtc contain weakly- to moderately-developed calcium carbonate horizons (Stage II+; Table 3) and yield profile mass carbonate values that range between 8.90 and 29.00 g/cm$^2$ (Table 3; Machette et al., 1997; Majkowski, 2009; Sion, 2015).

Qtd is a broad fill-cut terrace that is locally preserved between 6- and 4-km upstream from the Rio Grande (Fig. 3). Two small terrace remnants mapped in the upper 18- to 19-km section are tentatively correlated to Qtd based on height above the modern channel (~25 m). The broad tread of Qtd in the downstream section projects approximately 23 to 26 m above the modern channel, and terrace deposits are approximately 3-5 m thick (Machette, 1978). The terrace alluvium sits on top of exposed Pliocene basin-fill deposits of the Sierra Ladrones Formation (Machette, 1978), and the tread is covered by piedmont alluvium equivalent to unit "D" (Machette, 1978) that grades south towards the Rio Grande, west of San Acacia. Machette (1978) exclusively mapped piedmont deposits on this surface, but the presence of Rio Salado gravel lithologies was identified at the surface near the northern flank of the terrace tread. When projected to the Rio Salado, the heights of Qtd remnants on the northern edge of the broad terrace remnant systematically increase downstream. It is not clear whether or not Qtd is cut by any of the major faults in the valley due to the lack of terrace remnants near the faults. The age of Qtd is unknown, but must be older than Qtc. Machette et al. (1997) measured two profile mass carbonate values of 19.26 and 27.42 g/cm$^2$ from hand auger samples under this surface.

Qte forms a major fill terrace 28 to 50 m above the Rio Salado. Small discontinuous remnants approximately 10-m-thick line the southern flank of the valley between the Silver Creek fault (SiCF) and LPF (Fig. 3). Broad, continuous remnants north of the valley define two terrace levels that were not mapped separately by Machette (1978): higher $Qte_1$ and lower $Qte_2$, which are separated by an ~1- to 3-m riser in the hanging wall of the LBF. There, $Qte_1$ and $Qte_2$ are covered by sand sheets >1.5 m thick (Machette, 1976). Terrace alluvium thickness of $Qte_1$ is poorly constrained but is >20.5 m in one borehole (Machette, 1976). The thickness of Qte deposits east of the CF is unknown. Both Qte treads are cut by the LBF and exhibit differential offset. The $Qte_1$ tread is displaced by approximately 15 m, and the $Qte_2$ tread is displaced by approximately 8 m. The terrace treads are not offset by the west-down CF (Machette, 1978). Machette et al. (1997) described a Stage III carbonate morphology and measured a soil profile mass carbonate value of 21.86 g/cm$^2$ in one soil pit on $Qte_1$ (Table 3).

Qtf is a fill terrace that projects approximately 55 to 69 m above the modern channel. Alluvial thickness of Qtf deposits is variable across the LBF. Discontinuous remnants with alluvial thickness of 8- to 12-m line the northern flank of the valley in the footwall of the LBF. One borehole log requires Qtf deposits to have a minimum thickness of 22 m between the LBF and CF (Machette, 1976). Qtf deposits are approximately 10 m thick east of the CF. The strath of Qtf is carved into several geologic units that are juxtaposed by strands of the LPF. Upstream of the LPF, the strath is cut into Miocene playa beds of the Popotosa Formation. Between the LPF and LBF, the strath is primarily carved into deposits of a south-flowing axial stream (Machette, 1978). The strath is buried in a structural graben between the east-down LBF and the west-down CF. Qtf apparently is not cut by the LPF in this area. Qtf is offset by at least 15 m by the LBF based on direct measurements of Qte offset. The

TABLE 3. Estimated incision ages for Rio Salado terraces. Average incision ages are calculated based on the range of $Qte_2$ tread heights in the Rio Salado valley and the $^{36}$Cl age of the correlative "Airport surface" determined by Phillips et al. (2003). We also present ranges of pedogenic carbonate inventories and associated carbonate stage morphologies. [1]Machette et al. (1997); [2]Majkowski (2008); [3]Sion (2015).

| Terrace level | Tread height (m) | Airport surface incision age (ka) | Pedogenic carbonate inventories (g/cm$^2$) | Carbonate stage morphology |
|---|---|---|---|---|
| Qtg | 91-94 | 346 ±123 | 62.34[1] | III+ |
| Qtf | 53-68 | 235 ±105 | - | III |
| $Qte_1$ | 30-49 | 160 ±86 | 21.86[1] | III |
| $Qte_2$ | 28-42 | 122 ±18 | - | - |
| Qtd | 24-26 | 95 ±36 | 19.26-27.42[1] | III |
| Qtc | 5-18 | 52 ±39 | 8.90-29.00[1,2,3] | II+ |
| Qtb | 1-3 | 7 ±5 | - | I |

Qtf tread apparently is not cut by the CF, but this interpretation relies on the correlation of a small terrace remnant east of the CF on the northern flank of the valley (Fig. 5). Soil profile mass carbonate has not been measured on remnants of Qtf, but Machette (1978) reports moderately- to strongly-developed calcium carbonate horizons up to 1 m thick likely reflecting a Stage III carbonate morphology.

Qtg is a >24-m-thick fill terrace that forms the highest, oldest terrace in the valley (Machette, 1978). The tread of Qtg projects to a height approximately 88 to 94 m above the modern channel. One large remnant of Qtg is preserved on the north flank of the valley on the footwall of the east-down LBF (Fig. 4). Sierra Ladrones Formation deposits crop out beneath Qtg deposits in the footwall of the LBF. In the immediate hanging wall of the CF, Pliocene piedmont slope deposits (Tsp of Machette, 1978) crop out beneath alluvial "G" deposits. Strands of the LPF are apparently are buried by piedmont "G" deposits (Machette, 1978). The Qtg tread is offset by >34 m by the LBF, based on the associated scarp height on the Qtg surface. It is not clear whether or not the Qtg tread is cut by the CF. Machette (1978) correlated this surface to the aggradational top of the Sierra Ladrones Formation, however, the presence of an apparent terrace riser on the northern flank of Qtg (Fig. 4) suggests that the Qtg tread is inset into the high-stand surface and therefore younger than 800 ka. Machette et al. (1997) described a soil exposure in an alluvial "G" deposits west of the CF that projects approximately 67 m above the modern channel, noted a thick (>136 cm) Stage III carbonate horizon, and measured a profile mass carbonate of 62.34 g/cm$^2$.

## DISCUSSION

### Correlation and Estimated Ages of Rio Salado Terraces

We correlate our $Qte_2$ terrace to the 30-m-thick Rio Grande terrace of Love et al. (2009) and to the Segundo Alto terrace of Connell et al. (2007) (Table 4). Tread elevations of $Qte_2$ in the hanging wall of the LBF project to the elevation of a broad remnant of the "30-m terrace" at the Rio Grande junction (Fig. 5). Love et al. (2009) mapped nearly-continuous remnants of this terrace from San Acacia as far north as Veguita, NM. They also traced discontinuous remnants of the 30-m terrace south to Socorro where the 122±18-ka "Airport surface," a Socorro Canyon tributary terrace (Qvo3 of Chamberlin, 1999; T2 of Goldstein, 2001; dated by Phillips et al., 2003), projects to a similar elevation and provides a preliminary age estimate of $Qte_2$. The Segundo Alto terrace near Albuquerque, NM is composed of the 30- to 40-m-thick Los Duranes Formation, which buries 156±20-ka-old Albuquerque basalts and is buried by 98- to 110-ka-old Cat Hills basalts (Connell et al., 2007), placing the age of the Segundo Alto terrace within the age range of the Airport surface.

Connell et al. (2007) recognize a low terrace that may be correlative to our Qtc terrace. The Primero Alto terrace near Albuquerque, NM is composed of the 3- to 6-m-thick Arenal Formation and sits 15 m above the modern valley (Connell et al., 2007). We observe similar alluvial thickness, tread height and soil carbonate stage morphology in our Qtc terrace (Tables 1 and 3). This terrace has not been traced along the Rio Grande, however, Love et al. (2009) identified three minor, gravel-capped strath terraces that sit 7 to 12 m above the Rio Grande near the Rio Salado junction, but they attributed them to local discharge events and not to climatic or tectonic episodes.

Below we present inferred Rio Salado terrace ages based on estimated Rio Salado stream incision rates in the valley. We use the correlation of $Qte_2$ to the 122±18-ka-old Airport surface (Qvo3 of Chamberlin,1999; T2 of Goldstein, 2001; dated by Phillips et al., 2003) and the range of observed $Qte_2$ tread heights in the valley (Table 3) to estimate an average net incision rate of 0.30±0.1 m/kyr (propagated error from age estimate and range in terrace-tread height) since $Qte_2$ time. This incision rate suggests an age of ~346±123 ka for Qtg, the highest Rio Salado terrace. Machette (1978) correlated Qtg to the ~800 ka old basin fill top. We identified a potential Rio Salado terrace riser above Qtg, however (Fig. 4), suggesting that Qtg is inset into the top of the regional basin fill. This places Qtg somewhere between 346 and 800 ka old. We estimate ages of 235±105 ka for Qtf, 160±86 ka for $Qte_1$, 95±36 ka for Qtd, 52±39 ka for Qtc, and 7±5 ka for Qtb (Table 3). These estimates contain significant errors that result from propagating the error estimate given for the Airport surface, but also primarily due to the large range of observed tread heights for each terrace level.

TABLE 4. Preliminary correlation of Rio Salado terraces. Our $Qte_2$ terrace probably correlates with the "30-m terrace" of Love et al. (2009), which they traced from Veguita to Socorro. This correlation provides important age control for Rio Salado terraces, allowing for more regional correlation to the Segundo Alto terrace of Connell et al. (2007). Additional correlations are speculative, but our Qtc terrace probably correlates to the Primero Alto terrace of Connell et al. (2007) based on similar tread height, alluvial thickness and soil carbonate morphology.

| Rio Salado | Rio Grande at Albuquerque (Connell et al., 2007) | Rio Grande at San Acacia (Love et al., 2009) | Socorro Canyon (Chamberlin, 1999; Goldstein, 2001) |
|---|---|---|---|
| | Sunport, Las Huertas surfaces | | Las Cañas |
| Qtg | | | |
| Qtf | | | |
| $Qte_1$ | | | |
| $Qte_2$ | Segundo Alto | 30-m terrace | Qvo3/T2 |
| Qtd | | | |
| Qtc | Primero Alto | | Qvo4/T3 |
| Qtb | | | Qvo5/T4 |

### Mechanisms Controlling Rio Salado Terrace Gradients

We explore four mechanisms as end-member scenarios (Fig. 6a-d) that influence terrace gradients and can account for the dome-like geometry centered on the Loma Blanca fault. We also discuss how they relate to the configurations of the Rio Salado terraces. These mechanisms are: (1) base-level change due to climate fluctuations, (2) listric-style normal faulting, (3) domi-

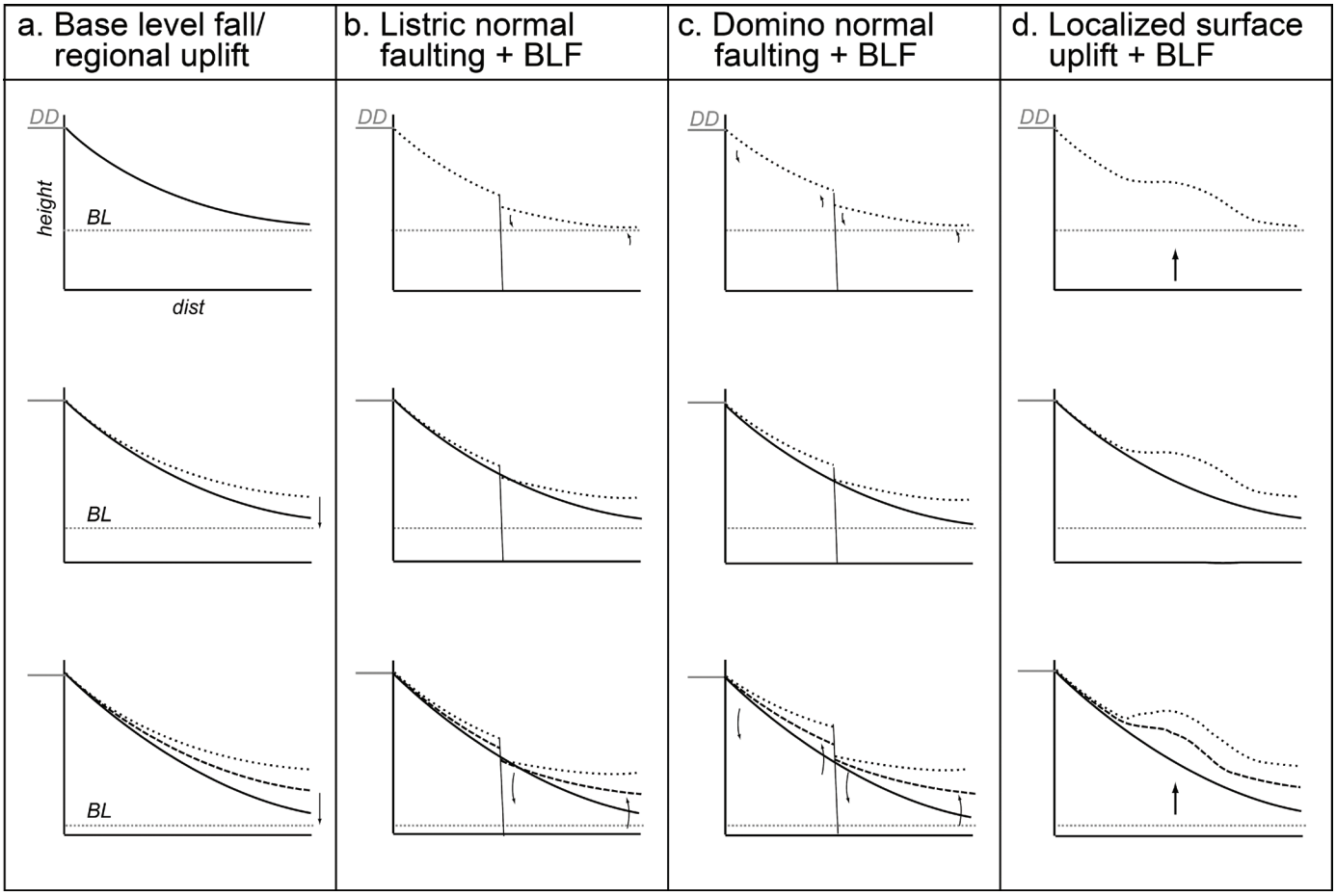



FIGURE 6. Mechanisms controlling Rio Salado terrace gradients. In all columns, the bold curve represents the height of a graded equilibrium stream bed as a function of distance downstream. DD indicates the drainage divide. Height of the DD is the same in all panels. BL is base level. Curved arrows indicate rotation due to faulting, downward arrows indicate base level fall, and upward arrows indicate surface uplift. Column (**a**) shows the expected terrace gradients through time as a result of periods of base level fall followed by periods of equilibrium. Terrace gradients in this scenario increase through time. Column (**b**) shows the expected terrace gradients after listric normal faulting causes back-tilting of the hanging wall. This is overprinted on the base level fall scenario. The result is increased back-tilting through time. Column (**c**) shows the expected terrace gradients after domino-style faulting. Terraces on the hanging wall and footwall are back-tilted by the same amount. Terraces are progressively back-tilted through time. Column (**d**) indicates the expected terrace gradients after surface uplift locally deforms a terrace. The result is an arched terrace geometry.

no-style normal faulting, and (4) localized surface uplift due to the presence of the Socorro magma body.

**Effects of Base-Level Change**

The Rio Grande axial river system locally acts as base level for the Rio Salado. The history of the Rio Grande is complex, but can be described in two major phases: (1) aggradation and basin filling followed by (2) valley entrenchment and partial valley backfilling. Before it became a fully integrated system, the Rio Grande drained into closed basins (Chapin and Cather, 1994; Connell et al., 2004). Basin filling eventually resulted in fluvial spillovers that ultimately lead to complete integration to the Gulf of Mexico in the middle Pleistocene (Gustavson, 1991; Galloway et al., 2000; Connell et al., 2004; Mack et al., 2006). The Rio Grande valley continued aggrading until incision began ~800 ka ago (Mack et al., 2006; Connell et al., 2013). Since then, the Rio Grande has episodically incised and partially back-filled its valley in concordance with glacial-interglacial cycles (e.g., Gile et al., 1981; Connell et al., 2007, 2013), resulting in net incision (except for the last 10-15 kyr, when it aggraded 20-25 m). Because the Rio Grande acts as local base-level control for its tributaries, incision of the Rio Grande lowers the base level of its tributaries, causing them to incise. If we assume that the elevation of the drainage divide at the upstream end of the tributary is constant through time, then the effect that base level fall has on the tributary stream is that of incision and increased stream gradient. This leaves behind a terrace level with a gradient that equals that of the paleo-stream before base level fall. Thus, we expect to see increased terrace gradients with decreasing terrace age, with associated profiles that converge upstream, if base-level fall acted as the primary mechanism of terrace formation (Fig. 6a).

**Effects of Normal Faulting**

A variety of normal fault styles are common in extensional terrains (Wernicke and Burchfiel, 1981). Two types of normal faults are potentially important in the lower reach of the Rio Salado (Fig. 6b-c). Listric normal faults are characterized by a

concave-up fault surface, decreasing dip with depth and tilting of the hanging wall block toward the fault and the presumably stable footwall block (Wernicke and Burchfiel, 1982). In contrast, planar domino-style normal faults (e.g., Morton and Black, 1975; Chamberlin, 1983) resemble a row of books falling over on a shelf, wherein the footwall, hanging wall and fault are all tilted by the same amount (Wernicke and Burchfiel, 1981; Axen, 1988). In addition, some domino-style normal faults are themselves listric, so cause more tilting of the hanging wall than of the footwall block or fault plane (Proffett, 1977). Both listric and domino-style normal faults were active in the early Rio Grande rift history (Chamberlin, 1983; Russell and Snelson, 1994; Baldridge et al., 1995). Late-rift, Plio-Pleistocene normal faults are common and generally dip steeply (≥60°) near the surface (Chamberlin, 1983; Machette et al., 1998). For example, the Cliff fault dips steeply where it is well exposed west of the Sevilleta NWR headquarters (unpublished data). Low-to-moderate angle normal faults also appear to be common in the rift (Ricketts et al., 2015). Normal faults of this type that cross the lower Rio Salado include the east-down Loma Peleda fault (LPF), which dips as little as 28° a few kms south of the Rio Salado (Machette, 1978), and the east-down Loma Blanca fault (LBF), which dips ~45° at the southern valley edge (unpublished data).

Terrace gradients in the hanging wall and footwall of the previously mentioned faults may shed light on the fault geometry. The LBF offsets several terrace levels in the Rio Salado valley by at least 15 m, but the LPF and CF apparently do not offset any of the mapped terraces (Fig. 5). If we observe strong back-tilting of terraces in the hanging wall block of the fault relative to the footwall block, listric normal fault geometries are expected (Fig. 6b). Domino faulting is expected if both the hanging wall and footwall are tilted by the same amount (Fig. 6c). Isostatic rebound has been documented in the footwall of large-displacement (10's of km), low-to-moderate angle normal and listric faults (e.g., Vening-Meinesz, 1950; Spencer, 1984; Wernicke and Axen, 1988). This process is likely negligible in the relatively small intra-rift faults of the Rio Salado valley because the length scales over which this is observed in the Basin-and-Range Province is much larger than observed here, and sedimentation in the footwall blocks is counteracting unloading of the hanging wall blocks.

**Surface Uplift due to the Socorro Magma Body**

Active surface uplift occurs above the northern two thirds of the Socorro magma body (Fig. 2; Fialko and Simons, 2001; Finnegan and Pritchard, 2009; Pearse and Fialko, 2010) and is probably affecting terrace elevations and gradients in the lower Rio Salado valley. The uplift pattern is approximately circular in map view, indicating surficial doming, and surface velocities may have remained roughly constant over the past ~100 years (Reilinger et al., 1980; Pearse and Fialko, 2010). InSAR data show maximum uplift in the Rio Salado valley of 1.8 ±0.2 mm/yr centered 10- to 15-km upstream of the Rio Salado from the Rio Grande. Differential uplift between this zone of maximum uplift and the west and east ends of the study area are ~1.3±0.2 mm/yr and ~0.5 mm/yr, respectively (Fig. 5; Finnegan and Pritchard, 2009; Pearse and Fialko, 2010).

This deformation pattern may cause arching of terraces in the lower Rio Salado valley (Fig. 5) if these rates persisted long enough to discern such an arch in the topographic data. We expect at least 15 cm of differential uplift in the Rio Salado valley over the (~100 yr) duration of observation, and 1.5-m differential uplift if the SMB crystallized over 1 kyr, as suggested by 1-D thermal models (Fialko and Simons, 2001). We would likely not be able to discern signals of this magnitude with our data set (accuracy ≤1 m), however, a signal resulting from several kyr of deformation (>5-m differential uplift) should be discernable. Arching would likely reflect tectonic deformation and not fluvial deposition, which was argued for a bulge in the Rio Grande profile (Ouchi, 1985; Finnegan and Pritchard, 2009), because there are no large tributaries (>40 km$^2$) in the study area that deposit appreciable amounts of sediment in this reach of the Rio Salado. Additionally, the modern stream profile does not show a bulge (Fig. 5). If the uplift pattern (and thus magma emplacement) is intermittent through time, we also expect older terraces to be increasingly arched (Fig. 6d).

**Comparison of Observed Terrace Gradients to End Member Models**

Comparison of our longitudinal profiles with those predicted by the models described above elucidate the most plausible climatic and tectonic mechanisms for the observed terrace gradients in the Rio Salado valley. We proceed from the youngest to oldest terrace.

The average gradient of Qtb is parallel to the modern stream grade (6.2 m/km; Table 1). There is no evidence of deformation related to either faulting or surface uplift, however several terrace remnants in the vicinity of Cañada Popotosa are higher above the channel than those elsewhere in the valley (Fig. 5). We attribute this to sedimentation from Cañada Popotosa.

Qtc is preserved throughout most of the study area. The tread of Qtc exhibits an arched geometry, where the gradient is gentler from 15- to 20-km distance upstream of the Rio Grande, levels out to a grade similar to the modern stream from 10-14 km, and becomes steeper than the modern stream grade from 1-8 km (Table 1; Fig. 5). This geometry cannot be due to fluvial processes because the erosional strath of the terrace mimics the arched geometry of the depositional tread (Fig. 5), indicating that the geometry is post-depositional. It is uncertain whether or not the LBF cuts the Qtc tread. Reconstructions made assuming that Qtc is cut by the LBF yield an abrupt thinning of terrace deposits in the hanging wall. Therefore, we prefer the interpretation that Qtc has not been cut by the LBF and was deformed by SMB-related surface uplift. If a period of SMB-related surface uplift deformed Qtc, it ceased before abandonment of Qtb.

Several small treads of Qtd are preserved in the hanging wall of the LBF and only two minor remnants were mapped in the footwall 18-km upstream from the Rio Grande junction (Fig. 5). Gradients in the footwall section could not be determined due to the lack of preservation. The tread of Qtd has a gradient of 4.1 m/km in the hanging wall of the LBF (Table 1), suggesting that it may be back-tilted by normal faulting (Fig.

5), but the Qtd tread does not yield SMB-related surface uplift. The projected hanging wall gradient of this surface is misleading, however, because the surface exhibits a strong north-south gradient in addition to the east-west gradient shown in Figure 5. The configuration of this terrace, therefore, is problematic so it does not provide useful tectonic constraints.

$Qte_2$ is well-preserved in the study area and is offset by the LBF (Fig. 5). The gradient of $Qte_2$ is less steep than the modern stream grade on the footwall of the LBF and has an average gradient 5.6 m/km (Table 1), consistent with each of the tectonic mechanisms discussed above. $Qte_2$ has a gradient of 5.4 m/km on the hanging wall, similar to that on the footwall. This is consistent with a domino, or possibly listric, fault geometry. The height of the riser between $Qte_1$ and $Qte_2$ is much greater on the footwall (~10 m) of the LBF than on the hanging wall (~2 m), consistent with LBF displacement occurring between abandonment of $Qte_1$ and $Qte_2$. The $Qte_2$ tread is not as dramatically arched as Qtc, but decreasing terrace height upstream from the LBF is consistent with SMB-related uplift.

The terrace-tread profiles of $Qte_1$ have average gradients of 5.6 m/km on the footwall of the LBF and 4.2 m/km on the hanging wall (Table 1). The terrace-tread gradients in the footwall are less steep than the modern stream grade (Fig. 5), consistent with each of the tectonic mechanisms above, but the gradient of $Qte_1$ depends on uncertain correlation to a small terrace remnant 8 km to the west. Given this uncertain correlation, the gradient of $Qte_1$ appears to be less steep in the hanging wall of the LBF relative to the footwall, which is more consistent with a listric fault geometry than domino normal faulting.

Terrace level Qtf is discontinuous in the study area, but many remnants are preserved. Qtf is offset by the LBF but apparently is not offset by the CF. The Qtf profile has average linear gradients of 5.9 m/km on the footwall of the LBF and 5.9 m/km on the hanging wall (Table 1), but this hanging wall gradient highly depends on the correlation of Qtf to a small remnant 3-4 km to the east. The footwall gradient is only slightly less steep than the modern channel (6.3 m/km). This is consistent with a gentler channel gradient during Qtf time, but may also result from footwall rotation due to domino-style faulting. The vertical distance between Qtf and $Qte_1$ on the hanging wall (and on the east side of the SMB-related arch) decreases to the east, indicating that these gradients could be explained by a period of SMB-related surface deformation after Qtg was abandoned. If a period of SMB-related surface uplift deformed Qtf, it ceased before $Qte_1$ was abandoned. If the small remnant mentioned above is not correlative to Qtf, however, the gradient of the Qtf tread in the hanging wall would be essentially zero ($3 \times 10^{-4}$ m/km), suggestive of strong back-tilting relative to its footwall counterpart, consistent with a listric fault geometry.

We calculate a poorly constrained gradient of 5.4 m/km (Table 1) from the single remnant of Qtg in the study area, which is notably less steep than the modern channel. Since the remnant is in the immediate footwall of the LBF, the apparent back-tilting can be the result of either base-level fall, domino-style faulting or uplift due to the SMB. A gentler stream gradient during Qtg time is probable, since base level has lowered since then due to Rio Grande incision. Because the remnant is in the immediate footwall of the LBF, isostatic uplift from listric faulting is also possible. Additionally, since there are no remnants of Qtg in the hanging wall, we cannot evaluate whether Qtg is differentially-tilted across the fault. The remnant is too small to make any observations regarding deformation due to SMB-related uplift, but since uplift is ongoing, it has likely been at least modestly deformed.

We cannot discount isostatic rebound as the mechanism controlling terrace steepening with decreasing terrace age. The terrace profiles in Cañada Alamosa of McCraw and Williams (2012) that are offset by the Willow Draw fault exhibit upwarps on the immediate footwall of the fault. This footwall deformation resembles isostatic footwall adjustment that is observed in faulted blocks of the basin and range (Wernicke and Axen, 1988), however the scale over which this apparent warping has been observed in Cañada Alamosa terraces is not consistent with footwall flexure. The 10-km distance of back-tilting of Rio Salado terraces on the footwall of the LBF is subtle (Fig. 5) but consistent with wavelengths expected in isostatic footwall adjustment (Wernicke and Axen, 1988). Thus, isostatic footwall uplift west of the LBF may have occurred in the lower Rio Salado Valley.

One can compare ranges of calculated paleo gradients of the Rio Salado at 800 ka with the expected magnitude of fault-block rotation. We observe a 15-m scarp on $Qte_1$ due to slip on the LBF. The hanging wall block extends 6 km east of the LBF to the CF, however, because the CF was not active during Qte time, this represents a minimum width of the hanging wall block. Thus, we compute a maximum of 2.5 m/km rotation as a first-order estimate due to domino-style normal faulting. Procedures of calculating ~800-ka paleo-slopes along the Rio Salado are discussed in Sion (2015). The estimated range of paleo-stream gradients (2.2-7.9 m/km) from these calculations is of similar order as expected from rotation due to domino-style faulting (2.5 m/km) and the total change in gradient between Qtg and the modern stream (2.8 m/km). Thus, the two mechanisms are indistinguishable with our current data.

We argue that a previous magma inflation event, similar in location to the current location of the SMB, can be interpreted using the terrace profiles of Qtc and Qtb, and that this event occurred between 52 and 7 ka. Both the tread and strath of Qtc are arched, and the tread of Qtc merges downstream with the tread of Qtb ~8 km above the junction with the Rio Grande (Fig. 5). We would expect that terraces on the downstream side of the uplift would never converge if constant base-level fall were overprinted by localized uplift (Fig. 6d). The maximum differential strath height is 7 m (12-14 km upstream of the Rio Grande). The coincidence between this arching pattern and the current deformation pattern (Fig. 5) lends support to this previous magma inflation event and also suggests that the SMB has not moved around significantly through time. The previous inflation event occurred between ~52 ka (the estimated age of Qtc) and the middle Holocene (the minimum age of Qtb).

We can also use our longitudinal terrace profiles to constrain the maximum duration of the prior inflation event (between 52 and 7 ka) and the current one. At current surface deformation rates (range of differential uplift of 0.5-1.3 m/ka

from the center of uplift along Rio Salado to the easternmost and westernmost Qtc remnants) it would take at least ~5-14 ka of constant uplift to cause a 7-m arch in Qtc (the maximum differential strath height). Qtb is not apparently arched. At current differential uplift rates, a deformation event of at least 1.5-4 ka would be necessary to create an arch in Qtb that exceeds the vertical accuracy and scatter of the digital elevation data from the Qtb remnants (1 m). Thus, the presently ongoing uplift event probably began <1.5-4 ka ago.

Thus, our observations favor two short-lived episode of SMB-related uplifts that are more rapid than rates of base-level fall, which would produce the observed terrace geometries. This is consistent with currently-observed SMB-related surface deformation rates, which are up to an order of magnitude larger than average Rio Salado stream incision rates inferred since the late Pleistocene (1.5-2.0 mm/yr vs. 0.30 ±0.10 mm/yr). The interpretation of two magmatic events, the first producing a maximum of 7 m of differential uplift over ~5-14 ka, and the second less than 1 m <1.5-4 ka, may explain why old composite surfaces in the Rio Grande valley (e.g., the Llano de Albuquerque and Llano de Manzano) do not record large magnitude displacements that would be expected over the SMB (see Finnegan and Pritchard, 2009) if uplift were continuous over time periods greater than tens of ka.

### Summary of the Evolution of Lower Rio Salado Terraces

The Rio Salado has episodically incised and partially backfilled its valley since Qtg time, creating six terrace levels that have gradients that increase with decreasing terrace age. Five of these terrace levels are tectonically deformed. The deformation is thought to be the result of both normal faulting and SMB-related surface uplift. The steepening of terrace gradients through time may be the result of base level fall, tectonic deformation or both. Below, we summarize the events that lead to the present configuration of the Rio Salado terraces.

The Rio Salado began incising pre-Qtg time. Sometime after a period of incision, backfilling resulted in deposition of Qtg. Another period of down-cutting was initiated after 346±123 ka ago, followed by backfilling. A speculative SMB-related surface deformation event may have caused the height of Qtf above $Qte_1$ to decrease eastward between abandonment of Qtf around 235±105 ka ago and abandonment of $Qte_1$ (160±86 ka), but this assumes correct correlation to a Qtf outlier east of most Qtf remnants. During this interval, the Rio Salado deposited the thick (>22 m) alluvial fill of $Qte_1$. The LBF offset $Qte_1$ and older terraces after abandonment of $Qte_1$. The LBF slipped ~7 m before formation of terrace $Qte_2$ (122±18 ka ago). This is documented by the differential heights of $Qte_1$ and $Qte_2$ on the footwall and hanging wall of the LBF. The Rio Salado incised into basin fill sediment, forming strath terraces Qtd (about 95±36 ka ago) and Qtc (about 52±39 ka ago). The arched geometry of Qtc relative to both Qtb and the modern stream grade strongly supports an episode of SMB-related surface deformation after the abandonment of Qtc. The LBF probably does not cut Qtc, indicating that the LBF was last active sometime before 52±39 ka ago. The geodetically-observed doming above the SMB (~100-year record) has not apparently deformed Qtb and likely represents another, very recent (<1.5-4 ka; see above), ongoing SMB-related deformation event.

## CONCLUSIONS

Improved terrace mapping, coupled with high-resolution longitudinal terrace profile analyses provide a framework for the terrace correlation in the lower Rio Salado. Six terrace levels are preserved in the valley. Terrace gradients systematically increase with decreasing terrace age, likely reflecting net incision of the Rio Grande or isostatic rebound of the LBF footwall. Longitudinal variations in terrace gradients and the presence of clear fault scarps suggest that the terraces have been tectonically deformed by faulting and surface uplift due to the SMB. Faulting appears to have ceased in the valley by Qtc-time and initiation of magma-body inflation happened sometime between Qtc- and Qtb-time This study is a progress report on a larger, ongoing terrace-mapping and correlation project in the Socorro area. The conclusions are preliminary and require additional field work, numerical dating and analysis for confirmation.

## ACKNOWLEDGMENTS

Discussions, in both the office and field, with D. Love and R. Chamberlin of the New Mexico Bureau of Geology and Mineral Resources have been very helpful. We thank Jon Erz and Glen and Ethel Freimuth of the Sevilleta National Wildlife Refuge for access to their land and permits to sample. This research was supported by grants EAR-1049966 and EAR-1348076 (GJA) from the National Science Foundation and by awards to BDS from the New Mexico Tech Graduate Student Association. Dave Love and Dan Koning provided helpful and constructive reviews that enhanced the manuscript.

## REFERENCES

Ake, J.P., and Sanford, A.R., 1988, New evidence for the existence and internal structure of a thin layer of magma at mid-crustal depths near Socorro, New Mexico: Seismological Society of America Bulletin, v. 78, p. 1335-1359.

Axen, G. J., 1988, The geometry of planar domino-style normal faults above a dipping basal detachment: Journal of Structural Geology, v. 10, p. 405-411.

Baldrige, W.S., Keller, G.R., Haak, V., Wendlandt, E., Jiracek, G.R., and Olsen, K.H., 1995, The Rio Grande rift, *in* Olsen, K.H., ed., Continental Rifts: Evolution, Structure, Tectonics: Amsterdam, Elsevier, Developments in Geotectonics, v. 25, p. 233-275.

Barnes, H., Spinelli, G.A., and Mozley, P.S., 2015, A 3-D view of field-scale fault-zone cementation from geologically ground-truthed electrical resistivity (abs.): American Geophysical Union Fall meeting, V53E-3154.

Bull, W.B., 1990, Stream-terrace genesis: implications for soil development, *in* Knuepfer, P.L.K., and McFadden, L.D., eds., Soils and Landscape Evolution: Amsterdam, Elsevier, p. 351-367.

Bull, W.B., 1991, Geomorphic Responses to Climatic Change: Oxford, Oxford University Press, 326 p.

Burbank, D.W., and Anderson, R.S., 2011, Tectonic Geomorphology: New York, John Wiley & Sons, 454 p.

Chamberlin, R.M., 1983, Cenozoic domino-style crustal extension in the Lemitar mountains, New Mexico: a summary: New Mexico Geological Society, Guidebook 34, p. 111-118.

Chamberlin, R.M., 1999, Preliminary geologic map of the Socorro 7.5-minute quadrangle: New Mexico Bureau of Geology and Mineral Resources, Open-file Geologic Map OF-GM 34, scale 1:24,000.

Chamberlin, R.M., Cather, S.M., Nyman, M.W., and McLemore, V.T., 2001, Preliminary geologic map of the Lemitar 7.5-minute quadrangle, Socorro County, New Mexico: New Mexico Bureau of Geology and Mineral Resources, Open-file Geologic Map OF-GM-38, scale, 1:24,000.

Connell, S.D, 2004, Geology of the Albuquerque Basin and tectonic development of the Rio Grande rift in north-central New Mexico, *in* Mack, G.H., and Gile, K.A., eds., The Geology of New Mexico – a Geologic History: New Mexico Geological Society, Special Publication 11, p. 359-388.

Connell S.D., Love, D.W., Dunbar, N.W., 2007, Geomorphology and stratigraphy of inset fluvial deposits along the Rio Grande valley in the central Albuquerque Basin, New Mexico: New Mexico Geology, v. 29, p. 13-31.

Connell, S.D., Smith, G.A., Geissman, J.W., and McIntosh, W.C., 2013, Climatic controls on nonmarine depositional sequences in the Albuquerque Basin, Rio Grande rift, north-central New Mexico: Geological Society of America, Special Paper 494, p. 383-425.

Denny, C.S., 1941, Quaternary geology of the San Acacia area, New Mexico: Journal of Geology, v. 49, p. 225-260.

Dethier, D.P., 2001, Pleistocene incision rates in the western United States calibrated using Lava Creek B tephra: Geology, v. 29, p. 783-786.

Dethier, D.P. and Reneau, S.L., 1995, Quaternary history of the western Epsañola Basin, New Mexico: New Mexico Geological Society, Guidebook 46, p. 289-298.

Fialko, Y. and Simons, M., 2001, Evidence for on-going inflation of the Socorro magma body, New Mexico, from Interferometric Synthetic Aperture Radar imaging: Geophysical Research Letters, v. 28, p. 3549-3552.

Finnegan, N.J. and Pritchard M.E., 2009, Magnitude and duration of surface uplift above the Socorro magma body: Geology, v. 37, p. 231-234.

Galloway, W.E, Ganey-Curry, P.E., Li, X., and Buffler, R.T., 2000, Cenozoic depositional history of the Gulf of Mexico basin: American Association of Petroleum Geologists Bulletin, v. 84, p. 1743-1774.

Gellis, A.C., Pavich, M.J., Bierman, P.R., Clapp, E.M., Ellevein, A., and Aby, S., 2004, Modern sediment yield compared to geologic rates of sediment production in a semi-arid basin, New Mexico: Assessing the human impact: Earth Surface Processes and Landforms, v. 29, p. 1359-1372.

George, N.K., Murray, M.H., Roy, M., Newman, A.V., Love, D.W., and Chamberlin, R.M., 2012, Horizontal deformation rates measured by ten years of GPS observations on the Socorro magma body, New Mexico, USA: Abstract T43C-2692 presented at the 2012 Fall Meeting, AGU, San Francisco, Calif., 3-7 Dec.

Gile, L.H., Hawley, J.W., and Grossman, R.B., 1981, Soils and geomorphology in the Basin and Range area of southern New Mexico: Guidebook to the Desert Project: New Mexico Bureau of Mines and Mineral Resources Memoir 39, 222 p.

Goldstein, H.L., 2001, Spatial variation in soils developed on fluvial terraces, Socorro basin, Rio Grande rift, central New Mexico [M.S. thesis]: Socorro, New Mexico Institute of Mining and Technology, 110 p.

Gosse, J.C., and Phillips, F.M, 2001, Terrestrial in-situ cosmogenic nuclides: theory and application: Quaternary Science Reviews, v. 20, p. 1475-1560.

Gustavson, T.C, 1991, Arid basin depositional systems and paleosols: Fort Hancock and Camp Rice Formations (Pliocene-Pleistocene), Hueco bolson, West Texas and adjacent Mexico: Bureau of Economic Geology, University of Texas at Austin, v. 198, 49 p.

Hawley, J.W., 1975, Quaternary history of Doña Ana County region, south-central New Mexico: New Mexico Geological Society, Guidebook 26, p. 139-150.

Koning D.J., Newell, D.L., Sarna-Wojcicki, A., Dunbar, N., Karlstrom, K., Salem, A., and Crossey, L., 2011, Terrace stratigraphy, ages, and incision rates along the Rio Ojo Caliente, north-central New Mexico: New Mexico Geological Society, Guidebook 62, p. 281-300.

Lavé, J., and Avouac, J.P., 2000, Active folding of fluvial terraces across the Siwaliks Hills, Himalayas of central Nepal: Journal of Geophysical Research, v. 105, p. 5735-5770.

Larsen, S., Reilinger, R., and Brown, L., 1986, Evidence of ongoing crustal deformation related to magmatic activity near Socorro, New Mexico: Journal of Geophysical Research, v. 91, p. 6283-6292.

Love, D.W., McCraw, D.J., Chamberlin, R.M., Reiter, M., Connell, S.D., Cather, S.M., and Majkowski, M., 2009, Progress report on tracking Rio Grande terraces across the uplift of the Socorro magma body: New Mexico Geological Society, Guidebook 60, p. 415-424.

Love, D.W., Reimers, R.F., Hawley, J.W., Johnpeer, G.D., and Bobrow, D.J., 1987, Summary of geotechnical investigations near Espanola, New Mexico, *in* Menges, C., ed., Quaternary tectonics, landform evolution, soil chronologies and glacial deposits – northern Rio Grande rift of New Mexico: Friends of the Pleistocene – Rocky Mountain Cell Field Trip Guidebook, p. 133-157.

Machette, M.N., 1976, Logs of drill holes, San Acacia 7.5-minute quadrangle, Socorro County, New Mexico: U.S. Geological Survey, Open-File Report 76-688, 20 p.

Machette, M.N., 1978, Geologic map of the San Acacia quadrangle, Socorro County, New Mexico: United States Geological Survey, Geologic Quadrangle Map GQ-1415, scale 1:24,000.

Machette, M.N., Long, T., Bachman, G.O., and Timble, N.R., 1997, Laboratory data for calcic soils in central New Mexico: Background information for mapping Quaternary deposits in the Albuquerque Basin: New Mexico Bureau of Mines and Mineral Resources, Circular 205, 63 p.

Machette, M.N., Personiums, S.F., Kelson, K.I., Haller, K.M., and Dart, R.L., 1998, Map of Quaternary faults and folds in New Mexico and adjacent areas: United States Geological Survey, Open-file Report 98-521, scale, 1:750,000.

Mack, G.H., Love, D.W., and Seager, W.R., 1997, Spillover models for axial rivers in regions of continental extension: the Rio Mimbres and Rio Grande in the southern Rio Grande rift, USA: Sedimentology, v. 44, p. 637-652.

Mack, G.H., Seager, W.R., Leeder, M.R., Perea-Arlucea, M., and Salyards, S.L., 2006, Pliocene and Quaternary history of the Rio Grande, the axial river of the southern Rio Grande rift, New Mexico, USA: Earth-Science Reviews, v. 79, p. 141-162.

Majkowski, L., 2009, Deflection of Rio Salado terraces due to uplift of the Socorro magma body, Socorro, New Mexico [M.S. thesis]: Socorro, New Mexico Institute of Mining and Technology, 88 p.

McCraw, D. J. and Williams, S. F., 2012, Terrace stratigraphy and soil chronosequence of Canada Alamosa, Sierra and Socorro counties, New Mexico: New Mexico Geological Society, Guidebook 63, p. 475-490.

Merritts, D.J., Vincent, K.R., and Wohl, E.E., 1994, Long river profiles, tectonism, and eustasy: A guide to interpreting fluvial terraces: Journal of Geophysical Research, v. 99, p. 14,031-14,050.

Molnar, P., Brown, E.T., Burchfiel, B.C., Qidong, D., Xianyue, F., Jun, L., Raisbeck, G.M., Jianbang, S., Hangming, W., Yiou, F., and Huichuan, Y., 1994, Quaternary climate change and the formation of river terraces across growing anticlines on the north flank of the Tien Shan, China: Journal of Geology, v. 102, p. 583-602.

Morton, W.H. and Black, R., 1975, Crustal attenuation in Afar, *in* Pilgar, A., and Rosler, A., eds., Afar Depression of Ethiopia, Inter-Union Commission on Geodynamics: International Symposium on the Afar Region and Related Rift Problems: Stuttgart, E. Schweizerbart'sche Verlagsbuchhandiung, p. 55-65.

New Mexico Bureau of Geology and Mineral Resources, 2003, Geologic map of New Mexico: New Mexico Bureau of Geology and Mineral Resources, scale 1:500,000.

Ouchi, S., 1985, Response of alluvial rivers to slow active tectonic movement: Geological Society of America Bulletin, v. 96, p. 504-515.

Pazzaglia, F.J., 2013. Fluvial terraces, *in* Wohl, E., ed., Treatise on Geomorphology, Fluvial Geomorphology: San Diego, Academic Press, p. 379–412.

Pazzaglia, F.J., and Wells, S.G., 1990, Quaternary stratigraphy, soils and geomorphology of the northern Rio Grande rift: New Mexico Geological Society, Guidebook 41, p. 423-430.

Pearse, J., and Fialko, Y., 2010, Mechanics of active magmatic intraplating in the Rio Grande Rift near Socorro, New Mexico: Journal of Geophysical Research, v. 115, p. 1-16.

Phillips, F.M., Ayarbe, J.P., Harrison, J.B.J., and Elmore, D., 2003, Dating rupture events on alluvial fault scarps using cosmogenic nuclides and scarp morphology: Earth and Planetary Science Letters, v. 215, p. 203-218.

Proffett, J.M., 1977, Cenozoic geology of the Yerington district, Nevada, and implications for the nature and origin of Basin and Range faulting: Geological Society of America Bulletin, v. 88, p. 247-266.

Reilinger, R.E., and Oliver, J.E., 1976, Modern uplift associated with a proposed magma body in the vicinity of Socorro, New Mexico: Geology,

v. 4, p. 583- 586.
Reilinger, R., Oliver, J., and Brown, L., 1980, New measurements of crustal doming over the Socorro magma body, New Mexico: Geology, v. 8, p. 291-295.
Reneau, S.L., 2000, Stream incision and terrace development in Frijoles Canyon, Bandelier National Monument, New Mexico, and the influence of lithology and climate: Geomorphology, v. 32, p. 171-193.
Ricketts, J.W., Karlstrom, K.E., and Kelley, S.A., 2015, Embryonic core complexes in narrow continental rifts: The importance of low-angle normal faults in the Rio Grande rift of central New Mexico: Geosphere, v. 11, p. 425-444.
Riihimaki, C.A, Anderson, R.S., and Safran, E.B., 2007, Impact of rock uplift on rates of late Cenozoic Rocky Mountain river incision: Journal of Geophysical Research, v. 112, p. 1-15.
Rockwell, T.K., Keller, E.A., Clark, M.N., and Johnson, D.L., 1984, Chronology and rates of faulting of Ventura River terraces, California: Geological Society of America Bulletin, v. 95, p. 1466-1474.
Russell, L.R., and Snelson, S., 1994, Structure and tectonics of the Albuquerque Basin segment of the Rio Grande rift: Insights from reflection seismic data: Geological Society of America, Special Paper 291, p. 83-112.
Schumm, S.A., and Parker, R.S., 1973, Implications of complex response of drainage systems for Quaternary alluvial stratigraphy: Nature, v. 243, p. 99-100.
Sion, B.D., 2015, Correlation and configuration of fluvial terrace deposits in the lower Rio Salado valley [M.S. thesis]: Socorro, New Mexico Institute of Mining and Technology, 47 p.
Spencer, J.E., 1984, Role of tectonic denudation in warping and uplift of low-angle normal faults: Geology, v. 12, p. 95-98.
Vening-Meinesz, F.A., 1950, Les “grabens” africains, resultat de compression ou de tension dans la croute terrestre: Bulletin of the Royal Colonial Institute of Belgium, v. 21, p. 539-552.
Wegmann, K.W., and Pazzaglia, F.J., 2002, Holocene strath terraces, climate change, and active tectonics: The Clearwater River basin, Olympic Peninsula, Washington State: Geological Society of America Bulletin, v. 114, p. 731-744.
Wernicke, B., and Axen, G.J., 1988, On the role of isostasy in the evolution of normal fault systems: Geology, v. 16, p. 848-851.
Wernicke, B., and Burchfiel, B.C., 1982, Modes of extensional tectonics: Journal of Structural Geology, v. 4, p. 105-115.



*Normal flow on Rio Puerco at Bernardo. Photo courtesy of Bonnie Frey.*